

## ELECTRONIC STRUCTURE OF TUNABLE MATERIALS MnAl AND MnGa

A. N. CHANTIS\*, D. O. DEMCHENKO\*, A. G. PETUKHOV\*, and W. R. L. LAMBRECHT\*\*

\*Department of Physics, South Dakota School of Mines and Technology, Rapid City, SD 57701-3995

\*\*Department of Physics, Case Western Reserve University, Cleveland, OH 44106-7079

### ABSTRACT

We present first-principle calculations of equilibrium lattice constants, band structures, densities of states and magnetocrystalline anisotropy energy for bulk MnAl and MnGa. The linear-muffin-tin-orbital (LMTO) method has been used within the framework of the local spin density approximation (LSDA). Both the atomic sphere approximation (ASA) and the full-potential (FP) versions of the LMTO method were employed. Calculations of the equilibrium structures were performed both for paramagnetic and ferromagnetic phases of MnAl and MnGa. The results of these calculations indicate that the large tetragonal distortion of the crystal structure is caused by the spin polarization of the electronic subsystem. The magnetocrystalline anisotropy energy per unit cell for MnAl and MnGa is shown to be 0.244 meV and 0.422 meV respectively. This is in good agreement with previous calculations and some experimental data. Magnetic moments, density of states and dependence of magnetocrystalline anisotropy energy on the lattice constant ratio  $c/a$  are also found to be in good agreement with previous results.

### INTRODUCTION

MnAl and MnGa films have been grown epitaxially on semiconductor substrates and have received a lot of attention due to their intriguing magnetic and magneto-transport properties such as unusual magnetic anisotropy and extraordinary Hall effect (EHE). Being ferromagnetic, these compounds show a great promise for merging magnetism with semiconductor technology. For both MnAl and MnGa magnetization measurements by means of vibrating sample magnetometry and EHE indicate perpendicular magnetization with a remnant magnetization of about 200 emu/cm<sup>3</sup> and EHE resistivity in the range of 4-8  $\mu\Omega$  and 0.5-4  $\mu\Omega$  respectively [1, 2, 3]. Both materials display a square-like hysteresis shape of the  $M-H$  and EHE curves and reasonable coercivity. In addition to this, the measured value of magnetic anisotropy constant for MnAl is about  $10^6 J/m^3$  at low temperatures. This means that MnAl and most likely MnGa exhibit rather strong magnetocrystalline anisotropy which is at least 10 to 100 times stronger than that of the other ferromagnetic materials such as Fe, Co or Ni [4].

The strong magnetic anisotropy and EHE in MnAl and MnGa create the possibility for future utilization of these materials in novel hybrid magnetoelectronic devices, such as non-volatile memory elements and spin-injection transistors [5, 6]. For the fabrication of these hybrid devices, it is important to perform predictive calculations of the magnetic and magneto-transport properties of MnAl/GaAs and MnGa/GaAs heterostructures. First-principle calculations of the electronic structures of bulk MnAl and MnGa materials is a necessary step in this direction. In particular, we would like to predict the easy magnetization axes and the values of magnetic anisotropy energy (MAE). Since the unusual magnetic anisotropy of these compounds is related to their structural anisotropy in the  $\tau$ -phase, our primary goal is to find equilibrium atomic structures of  $\tau$ -MnAl(Ga) which are characterized by certain tetragonal distortions. Moreover, we would like to explore the interplay between spin polarization, structural distortion, and magnetic anisotropy. Despite of a number of important previous works on the electronic structure of MnAl and MnGa [7, 8] the first-principle determination of their equilibrium atomic structure has not yet been done. Here we report the results of our calculations of basic electronic, magnetic and structural properties of these materials.

### COMPUTATIONAL METHOD

MnGa and MnAl are both binary transition metal alloys, with CuAu-type tetragonal structure and experimentally measured lattice constants  $\bar{a}=0.390$  nm,  $\bar{c}=0.362$  nm and  $\bar{a}=0.393$  nm,  $\bar{c}=0.356$  nm respectively. This structure can be represented as two simple tetragonal sublattices of Mn and Al (or tetragonally distorted CsCl structure) with another set of lattice parameters  $a = \bar{a}/\sqrt{2}$  and  $c = \bar{c}$ . In the discussion that follows we will mostly refer to this structure as to a *reduced* structure with lattice parameters  $a$  and  $c$ . All calculations were performed in the framework of the local spin density approximation (LSDA) and the linear-muffin-tin-orbital method (LMTO) in both its atomic sphere approximation (ASA) and full-potential (FP) versions. The latter was employed in the calculation of the equilibrium structure constants.

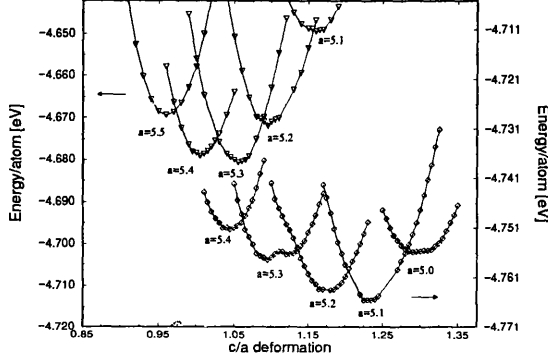


Figure 1: Total energies versus  $c/a$  for MnAl. Diamonds: spin-polarized calculations; triangles: non-spin-polarized calculations.

In this case no spherical approximations can be made for the interstitial potential. Also the close packing of these particular structures allows the method to work with relatively high accuracy. Spin polarized and non-spin polarized equilibrium structure calculations were performed for both MnAl and MnGa.

Band structure, density of states and magnetic anisotropy energy calculations were performed with the LMTO-ASA method. In these calculations Ga 3d states in MnGa were treated as core orbitals. The density of states was calculated by means of the tetrahedron method on a regular mesh of 1000 points in the Brillouin zone. This was found to be sufficient to achieve self-consistency in the charge density with high accuracy. For the calculation of the magnetic anisotropy energy we used the force theorem, according to which, the MAE can be obtained as a difference of sums over occupied eigenvalues of one-electron Kohn-Sham equations corresponding to different directions of the magnetization [4]:

$$\Delta E(\hat{n}) = \sum_{i,\vec{k}}^{occ} \epsilon_i(\hat{n}, \vec{k}) - \sum_{i,\vec{k}}^{occ} \epsilon_i(\hat{n}_0, \vec{k}) \quad (1)$$

where  $\hat{n}$  is the unit vector in the direction of magnetization and  $\hat{n}_0$  is the unit vector corresponding to the magnetization in [001] direction. To rotate the direction of magnetization we introduced a rotation matrix which performed a unitary transformation on spin-orbit part of the LMTO Hamiltonian. In this way we calculated the MAE as the aforementioned difference between the band energies for the magnetizations in the [100] and [001] directions in the reduced structure. The Brillouin zone integration was performed with the tetrahedron method on a regular mesh of 13824 sample points.

Table I: Equilibrium lattice constants, magnetic anisotropy energy (MAE), and magnetic moments (in  $\mu_B$ )

Compound	$a$ (Å), SP.	$a$ (Å), non-SP.	$c/a$ SP	$c/a$ non-SP	MAE (meV/unit cell)	$\mu_{Mn}$	$\mu_{Al}, \mu_{Ga}$
MnAl	2.699	2.804	1.23	1.06	0.244	-2.192	0.041
MnGa	2.540	2.752	1.46	1.11	0.422	-2.274	0.065

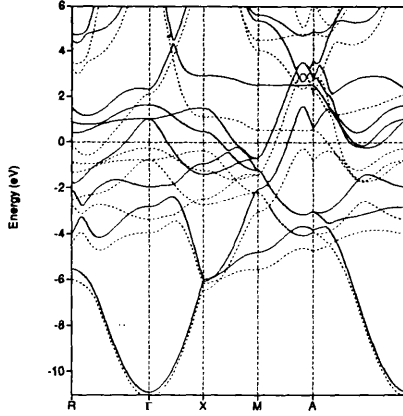


Figure 2: Spin-polarized band structure of MnAl

## RESULTS

### MnAl

Fig. 1 shows the results of non-spin polarized and spin-polarized equilibrium structure calculations for MnAl. In Table I we summarize all of the obtained results. The calculated lattice parameters are  $a=2.699$  Å,  $c=3.319$  Å and  $a=2.804$  Å,  $c = 2.972$  Å from spin-polarized and non-spin-polarized calculations respectively. The energy difference between non-spin-polarized and spin polarized states is 85 meV/atom. The non-spin-polarized calculated value of lattice parameter  $a$  is closer to the experimental one. In fact, the difference between non-spin-polarized calculated and the experimental value is within the ordinary limits given by all other similar calculations. However the non-spin-polarized calculations fail to predict the correct value for the crystal deformation parameter,  $c/a$ . This value is more accurately predicted by spin-polarized calculations. This fact clearly indicates that the deformation of the crystal is caused mainly by its magnetization.

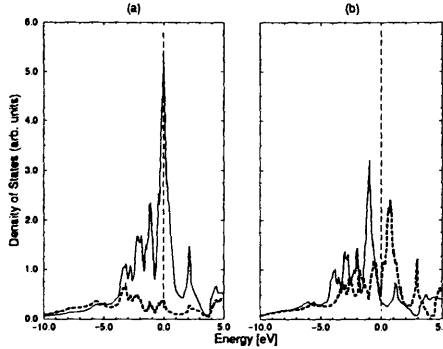


Figure 3: Density of states in MnAl: (a) non-spin-polarized calculations (solid line-Mn, dashed line-Al); (b) spin-polarized calculations (solid line-majority spins, dashed line-minority spins).

Fig. 2 shows the results of spin-polarized band structure calculations for MnAl. The symbols R,  $\Gamma$ ,

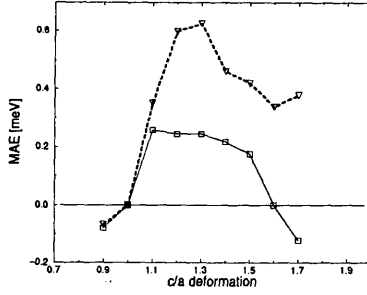


Figure 4: MAE versus deformation  $c/a$ , at equilibrium  $a$ , for MnGa(dashed line) and MnAl(solid line).

X, M, and A stand for the  $(0, \frac{1}{2}, \frac{1}{2})$ ,  $(0,0,0)$ ,  $(0, \frac{1}{2}, 0)$ ,  $(\frac{1}{2}, \frac{1}{2}, 0)$  and  $(\frac{1}{2}, \frac{1}{2}, \frac{1}{2})$  symmetry points in the MnAl Brillouin zone respectively. It is found that there is no band gap at the Fermi level and that a large exchange splitting of about 2 eV exists between Mn 3d states with opposite spins. Fig. 3a shows the non-spin polarized density of states (DOS) for MnAl. The DOS of Mn has a sharp maximum at the Fermi level, which leads us to expect that MnAl is ferromagnetic.

The spin-polarized DOS for MnAl is shown in Fig. 3b. The long tail in the range between -10 and -5 eV is mainly due to Al  $s$  states and Mn  $s$  states. The Al  $p$  states give a small contribution to the density of states, in the region adjacent to -5 eV while Mn  $d$  states are spread all over the plotted range and have the largest contribution in the range between -2 and 2 eV, where the total density of states almost coincides with Mn  $d$ -DOS. The calculated magnetic moments for Mn and Al are  $-2.192 \mu_B$  and  $0.042 \mu_B$  respectively. These values are slightly higher than the experimental ones [9], but the stoichiometry of the measured samples differs from the ideal one, for which all calculations are made.

The results of magnetocrystalline anisotropy energy calculations for both MnAl and MnGa are shown in Fig. 4 and Table I. At equilibrium, the MAE for MnAl is 0.244 meV per unit cell. This value is in good agreement with previous calculations and corresponds to  $\hat{n}$  in the [100] direction of the tetragonally distorted reduced crystal structure of MnAl or MnGa (see Eq.(1)). This means that in bulk MnAl, the axis of easy magnetization lies in the  $c$ -plane rather than in  $x, y$ -plane. Within the accuracy of our calculations it is impossible to predict the exact direction of the easy magnetization axis in the  $c$ -plane. The calculated value of the MAE, leads to the value  $1.4 \times 10^6 \text{ J/m}^3$  for the magnetic anisotropy constant  $K_u$  which is close to the measured value as well. The dependence of MAE upon the deformation  $c/a$ , indicates that the easy magnetization axis turns from the  $c$ -plane to the  $x, y$ -plane whenever the deformation  $c/a$  is smaller than 1 or larger than 1.6.

### MnGa

For MnGa we have almost the same picture with the exception that the obtained MAE, 0.422 meV per unit cell, is almost two times larger. This leads to a magnetic anisotropy constant  $K_u$  of  $2.6 \times 10^6 \text{ J/m}^3$ . Unfortunately, we are not aware of any experimental data for the magnetic anisotropy constant of this material. The dependence of MAE on the  $c/a$  also differs considerably from that obtained for MnAl. In Fig. 4 it is seen that the easy magnetization axis turns from the  $c$ -plane to the  $x, y$ -plane only when  $c/a$  is below 1. Another interesting fact is that the deformation in the equilibrium structure is also much greater than that of MnAl. The difference between spin polarized calculated and non-spin polarized calculated equilibrium  $c/a$  for MnGa is about two times larger than that in MnAl. This fact and the fact that the MAE for MnGa is also about two times larger than that of MnAl is a clear indication that the tetragonal deformation and the magnetic anisotropy are closely related to each other.

The results of the equilibrium structure calculations are presented in Fig. 5. As in MnAl, it is seen that while non-spin-polarized calculations give accurate value of the lattice constant  $a$  they fail to predict the correct value of the deformation parameter  $c/a$ . Again, this value is more accurately predicted by spin-polarized calculations. The calculated DOS for the non-magnetic and ferromagnetic states, are shown in

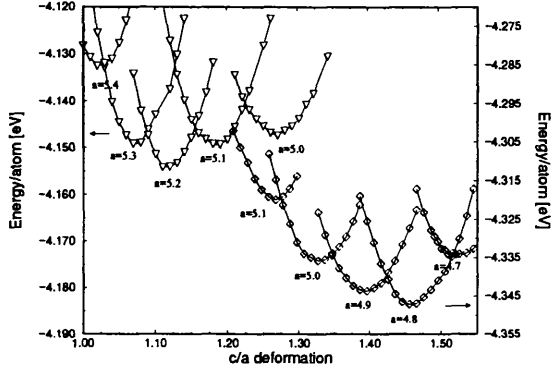


Figure 5: Total energies versus  $c/a$  for MnGa. Diamonds: spin-polarized calculations; triangles: non-spin-polarized calculations.

Fig. 6a and Fig. 6b respectively. Dispersion curves for the ferromagnetic phase are shown in Fig. 7. The calculated equilibrium lattice constants and magnetic moments are shown in Table I.

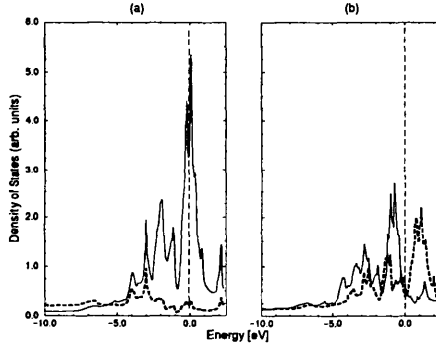


Figure 6: Density of states in MnGa: (a) non-spin-polarized calculations (solid line-Mn, dashed line-Ga); (b) spin-polarized calculations (solid line-majority spins, dashed line-minority spins).

## CONCLUSIONS

We have performed several first-principle calculations of the magnetic and electronic properties of bulk MnAl and MnGa. Along with these, we have performed equilibrium structure calculations for paramagnetic and ferromagnetic phases of these materials. The obtained results for magnetic moments, density of states, band structure and magnetocrystalline anisotropy energy are in good agreement with experimental data and previous calculations. The MAE for MnGa is twice as large as that in MnAl. The lattice deformation of MnGa in the ferromagnetic state is also two times larger than that of MnAl. This shows how closely related are the structural deformation and the magnetic anisotropy.

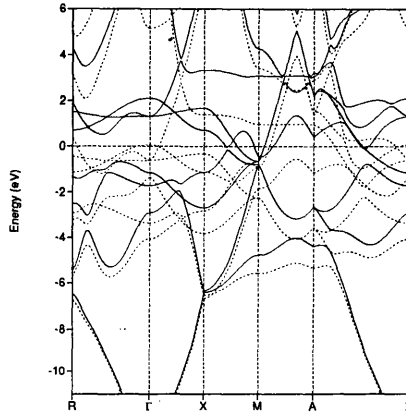


Figure 7: Spin polarized band structure of MnGa

## ACKNOWLEDGEMENTS

This work was supported by the AFOSR grant No. F49620-96-1-0383.

## REFERENCES

1. M. Tanaka, J.P Harbison, T. Sands, B. Philips, T. L. Cheeks, V. G. Keramidas, *Appl. Phys. Lett.* **62**, 1565 (1993).
2. J. De Boeck, R. Oosterholt, A. Van Esch, H. Bender, C. Bruynseraede, C. Van Hoof and G. Borghs, *Appl. Phys. Lett.* **68**, 2744 (1996).
3. W. Van Roy, H. Bender, C. Bruynseraede, J. De Boeck, G. Borghs, *J. Magn. Magn. Mater.* **148**, 97 (1995).
4. G. H. Daalderop et al., *Phys. Rev. B* **41**, 11919 (1990).
5. G. A. Prinz, *Science* **250**, 1092 (1990).
6. J. De Boeck, T. Sands, J. P. Harbison, A. Scherer, H. Gilchrist, T. L. Cheeks, M. Tanaka and V. G. Keramidas, *Electronics Lett.* **29**, 421 (1993).
7. A. Sakuma, *J. Phys. Soc. Japan* **63**, 1422 (1994).
8. A. Sakuma, *J. Magn. Magn. Mater.* **187**, 105 (1998).
9. N. I. Vlasova, G. S. Kandaurova, YA. S. Shur and N. N. Bykhanova, *Phys. Met. Metall.* **51**, 1 (1981).